Eur. J. Biochem. **267**, 1390–1396 (2000) © FEBS 2000

Structure and dynamics of lipid-associated states of apocytochrome *c*

Elzbieta A. Bryson[1], Saffron E. Rankin[1], Erik Goormaghtigh[2], Jean-Marie Ruysschaert[2], Anthony Watts[3] and Teresa J. T. Pinheiro[1]

[1]*Department of Biological Sciences, University of Warwick, Coventry, UK;* [2]*Laboratoire de Chimie-Physique des Macromolécules aux Interfaces, Université Libre de Bruxelles, Belgium;* [3]*Biomembrane Structure Unit, Department of Biochemistry, University of Oxford, UK*

Apocytochrome *c* (apocyt *c*), which in aqueous solution is largely unstructured, acquires an α-helical conformation upon association with lipid membranes. The extent of α-helix induced in apocyt *c* is lipid-dependent and this folding process is driven by both electrostatic and hydrophobic lipid–protein interactions. The structural and dynamic properties of apocyt *c* in lipid membranes were investigated by attenuated total reflection Fourier transform infrared spectroscopy combined with amide H–D exchange kinetics. Apocyt *c* acquires a higher content of α-helical structure with negatively charged membranes than with zwitterionic ones. For all membranes studied here, the helices of these partially folded states of apocyt *c* have a preferential orientation perpendicular to the plane of the lipid membrane. The H–D exchange revealed that a small fraction of amide protons of apocyt *c*, possibly associated with a stable folded domain protected by the lipid, remained protected from exchange over 20 min. However, a large fraction of amide protons exchanged in less than 20 min, indicating that the helical states of apocyt *c* in lipid membranes are very dynamic.

Keywords: attenuated total reflection Fourier transform infrared (ATR FTIR) spectroscopy; dynamics; H–D exchange kinetics; protein folding; stability.

Apocytochrome *c* is the haem-free precursor of the intermembrane mitochondrial protein cytochrome *c* (cyt *c*). The precursor protein is synthesized on free cytoplasmic ribosomes and has to cross the outer mitochondrial membrane to reach the intermembrane space, where cyt *c* functions as an electron carrier. The import pathway of apocyt *c* into mitochondria differs from those followed by other mitochondrial proteins. Apocyt *c* does not have a cleavable N-terminal presequence, and it does not require ATP or a transmembrane potential for the translocation (reviewed in [1]). Instead, it can spontaneously insert and, at least partially, cross model lipid membranes [2,3] and the outer mitochondrial membrane [4,5].

In contrast with the native holoprotein, apocyt *c* is largely an unstructured polypeptide in solution [6,7] with a residual amount of α-helix likely to be associated with the C-terminus [8]. However, binding of apocyt *c* to lipid membranes has been shown to induce the folding of apocyt *c* into an α-helical structure [9–11]. The α-helix content depends on the lipid type and protein to lipid molar ratio. Negatively charged lipid vesicles and micelles have been found to fold the protein to an α-helical state which resembles that of native cyt *c* in solution [11,12]. In contrast, zwitterionic vesicles are less effective at folding apocyt *c* [11,13]. CD measurements of the orientation of different fragments of apocyt *c* in lipid membranes revealed that the N-terminal and C-terminal helices have a preferential orientation perpendicular to the plane of saturated lipid membranes and parallel to unsaturated lipid membranes [13].

Despite the large number of studies devoted to unravelling the mechanism of translocation of apocyt *c* through mitochondrial or model membranes, this process is not fully understood at the molecular level. In particular, we have been interested in understanding the role of lipid-associated partially folded states of apocyt *c* in membrane insertion and translocation. To this end, we have investigated the folding kinetics of apocyt *c* induced by negatively charged lipid membranes [14] and zwitterionic ones [15]. These studies have shown that the folding kinetic pathway of apocyt *c* in lipid membranes depends on the lipid headgroup charge. In negatively charged lipid membranes, the folding of apocyt *c* involves an early compact intermediate before membrane insertion, whereas in zwitterionic ones, folding of apocyt *c* occurs via more extended helical conformations. These results have led us to propose that lipid-associated partially folded states of apocyt *c* may play a role in the molecular mechanism of insertion and/or translocation of apocyt *c* across lipid membranes. However, further structural and dynamic studies of folded states of apocyt *c* in lipid membranes are required to understand their potential role in membrane insertion and/or translocation.

Here we have employed attenuated total reflection Fourier transform infrared (ATR FTIR) spectroscopy to characterize the structural properties of apocyt *c* in negatively charged and zwitterionic lipid membranes. Negatively charged membranes show a tendency to induce more α-helical structure than zwitterionic ones. The helices in apocyt *c* were found to adopt a

Correspondence to T. J. T. Pinheiro, Department of Biological Sciences, University of Warwick, Gibbet Hill Road, Coventry CV4 7AL, UK.
Fax: + 44 2476 523 568, Tel.: + 44 2476 528 364,
E-mail: tp@dna.bio.warwick.ac.uk

Abbreviations: apocyt *c*, apocytochrome *c*; ATR, attenuated total reflection; cyt *c*, cytochrome *c*; DMPC, dimyristoylphosphatidylcholine (1,2-dimyristoyl-*sn*-glycero-3-phosphocholine); DMPG, dimyristoylphosphatidylglycerol [1,2-dimyristoyl-*sn*-glycero-3-phospho-*rac*-(1-glycerol)]; DPPC, dipalmitoylphosphatidylcholine (1,2-dipalmitoyl-*sn*-glycero-3-phosphocholine); DPPG, dipalmitoylphosphatidylglycerol [1,2-dipalmitoyl-*sn*-glycero-3-phospho-*rac*-(1-glycerol)]; FTIR, Fourier transform infrared.

(Received 6 September 1999; revised 3 December 1999, accepted 6 January 2000)

preferential orientation perpendicular to the plane of the membrane. The dynamic properties of apocyt *c* in lipid membranes were studied by the H–D exchange kinetics of amide protons. A large fraction of amides (up to 90%) were found to exchange in less than 20 min, indicating that these helical states of apocyt *c* in lipid membranes are very dynamic. A smaller fraction of protected amides were correlated with a more stable folded domain possibly inserted into the lipid membrane.

MATERIALS AND METHODS

Materials

Horse heart cyt *c* (type VI), dipalmitoylphosphatidylcholine (1,2-dipalmitoyl-*sn*-glycero-3-phosphocholine; DPPC) and dipalmitoylphosphatidylglycerol [1,2-dipalmitoyl-*sn*-glycero-3-phospho-*rac*-(1-glycerol); DPPG] were purchased from Sigma Chemical Co. (St Louis, MO, USA). Dimyristoylphosphatidylcholine (1,2-dimyristoyl-*sn*-glycero-3-phosphocholine; DMPC) and dimyristoylphosphatidylglycerol [1,2-dimyristoyl-*sn*-glycero-3-phospho-*rac*-(1-glycerol); DMPG] were from Avanti Polar Lipids, Inc. (Birmingham, AL, USA).

Protein purification

Horse heart cyt *c* was purified using the procedure of Brautigan *et al*. [16]. Apocyt *c* was prepared by chemically removing the haem group of cyt *c* as described by Fisher *et al*. [7]. The protein was purified by a modified version of the procedure reported by Hennig & Neupert [17] as described previously [11]. It was stored in aliquots at −20 °C, thawed and kept on ice on the day of the measurements to prevent protein aggregation. The concentration of purified apocyt *c* was determined spectrophotometrically using a molar absorption coefficient of 10 580 $M^{-1}\cdot cm^{-1}$ at 277 nm [6].

Sample preparation

Small unilamellar vesicles were prepared by hydration of the required amounts of lipid with 2.5 mM potassium phosphate buffer, pH 7.0, followed by sonication in a Branson 1200 bath sonicator until a clear suspension was obtained (typically ≈ 3 h). Aqueous solutions of apocyt *c* in 2.5 mM potassium phosphate buffer, pH 7.0, were mixed with the desired vesicles to final concentrations of 4 mM lipid and 40 μM protein. The mixture was incubated for 10 min at 30 ± 1 °C, and an aliquot of 50 μL was applied to a 50 × 20 × 2 mm germanium plate (Harrick, Ossining, NY, USA). Thin films were obtained by slow evaporation of the deposited sample under a N_2 stream. This procedure results in oriented lipid multilayers with acyl chains approximately perpendicular to the surface of the plate [18]. Protein films of apocyt *c* and cyt *c* without lipid, and lipid films without protein, were prepared in a similar manner from their buffer solutions. Lipid–protein samples had an excess lipid, with a lipid to protein molar ratio of 100 : 1.

ATR FTIR spectra

ATR FTIR spectra were recorded on a Bruker IFS-55 infrared spectrometer equipped with a liquid-nitrogen-cooled MCT (mercury cadmium tellurium) detector. Samples were sealed within the ATR plate holder in a vertical ATR configuration, with an angle of 45° between the incident beam and the germanium plate, producing 25 internal reflections. The spectrometer was continuously purged with air dried through a silica gel column. Spectra were recorded using light polarized in the direction parallel (∥) and perpendicular (⊥) to the plane of incidence. Typically, 64 scans were averaged per spectrum. Dichroic spectra were obtained by subtracting the spectra recorded with ⊥ polarized light from the spectra recorded with ∥ polarized light, with a weight coefficient R_{iso}, which is defined as the ratio of integrated intensity of the lipid carbonyl band in spectra recorded at ∥ and ⊥ polarizations [19]. All spectra were recorded with a resolution of 2 cm^{-1}, and measurements were performed at room temperature (≈ 26 °C inside the sample chamber).

The contribution from atmospheric water was subtracted from all spectra, as described in [20]. This procedure eliminates most but not all such contributions, and spectra were further corrected using a weighted coefficient based on the integrated area between 1562 and 1555 cm^{-1}. Weighted lipid spectra (based on the integrated area of the lipid carbonyl peak) were subtracted from the spectra of protein–lipid samples. Final spectra were smoothed by apodization with a 4-cm^{-1} full width at half height Gaussian line shape. Protein secondary structure was determined by self-deconvolution of spectra [21,22] and band assignments in deconvoluted spectra were made as described by Cabiaux *et al*. [23].

Hydrogen–deuterium exchange

Samples were deuterated by subjecting them to a stream of D_2O-saturated N_2 gas inside the sealed sample holder. The course of sample deuteration was monitored by acquiring FTIR spectra at various time points (*t*) sampled over a total exchange time of 20 min. Spectra were first recorded using ∥ polarized light followed by collection with ⊥ polarized light. For each polarization, 20–32 scans were averaged, and the total acquisition time at each polarization was 13–16 s. Thus, for the analysis of the exchange kinetic data (% deuteration vs *t*), *t* was taken as the value in the middle of the acquisition time for each polarization. Spectra at $t = 0$ (fully protonated sample) were recorded before initiating H–D exchange.

The kinetics of H–D exchange of amide protons was followed by monitoring the decrease in the integrated area of the amide II band in spectra recorded with ∥ and ⊥ polarized light. As the overall intensity of the spectra decreases as a result of the swelling of a sample exposed to D_2O-saturated N_2 gas, the area of the amide II was normalized to the area of the amide I band. Protein–lipid spectra were corrected for the lipid contributions, as described in the previous section. The relative area of the amide II band (i.e. the ratio of the area of the amide II band to the area of the amide I band) was then divided by the initial value ($t = 0$; fully protonated sample) of the relative area of amide II to give the fraction of protonated residues (a_H). The fraction of deuterated amides (a_D) was calculated as $a_D = 1 - a_H$. All H–D exchange curves were fitted to a minimum number of exponential terms using non-linear least-squares analysis with IGOR (Wavemetrics Inc., Lake Oswego, OR, USA).

RESULTS

Structure of apocyt *c* in lipid membranes

FTIR spectra were recorded with ∥ and ⊥ polarized light before and after 20 min of deuteration. The use of polarized light enabled the orientation of protein secondary structure elements to be determined. Deuteration of the samples allowed a

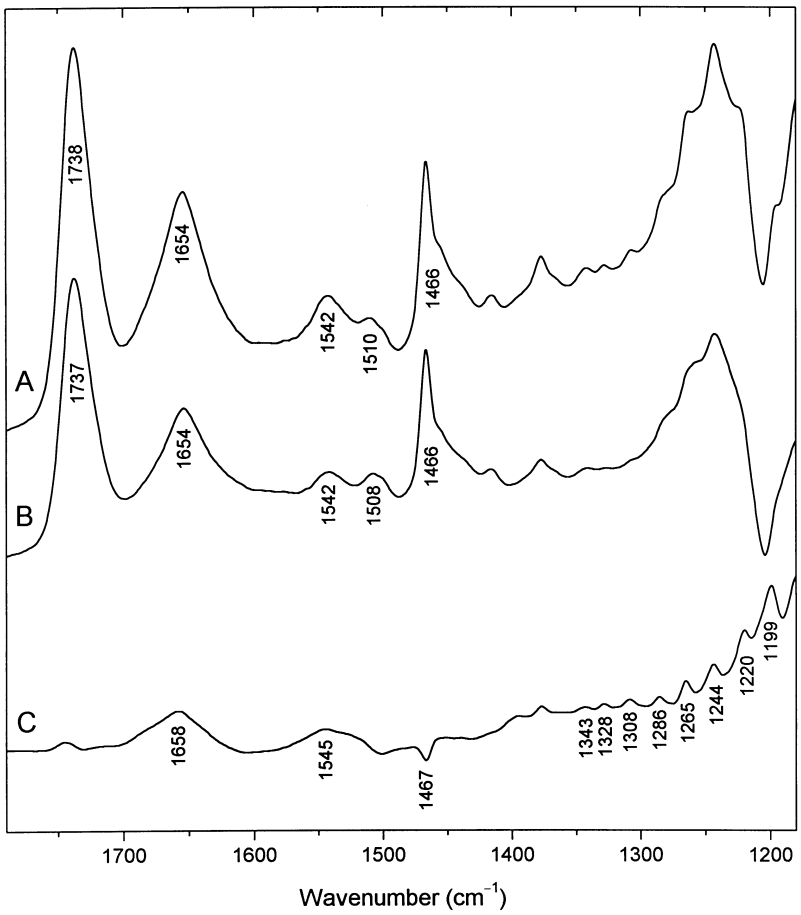

Fig. 1. FTIR spectra of apocyt *c* in the presence of DPPG. Spectra A and B were obtained with ∥ and ⊥ polarized light, respectively. Spectrum C represents a dichroic spectrum obtained by subtracting spectrum B from spectrum A with a weight coefficient R_{iso} of 1.36 used to zero the area of the lipid carbonyl peak. The wavenumbers of the main bands are indicated for lipid carbonyl stretching, ≈ 1738 cm^{-1}; protein amide I, 1654 cm^{-1}; protein amide II, 1508–1542 cm^{-1}; lipid scissoring peak, 1466 cm^{-1}; and the lipid $\gamma_w(CH_2)$ progression of bands, 1180–1350 cm^{-1}.

distinction between contributions from α-helix and random coil structures to be made, which in a protonated protein have very similar frequencies. Usually, brief (a few minutes) deuteration is sufficient to shift the random coil band to lower frequencies away from the α-helix band [24]. FTIR spectra were measured for apocyt *c* with zwitterionic membranes of DMPC and DPPC and with negatively charged membranes of DMPG and DPPG. Typical spectra are shown in Fig. 1 for apocyt *c* with DPPG membranes. Amide I and amide II bands arising from the protein can be seen near 1654 and ≈ 1508–1542 cm^{-1}, respectively. Lipid ester carbonyl stretching band and the so-called CH_2 scissoring band are present near 1738 cm^{-1} and 1466 cm^{-1}, respectively. The $\gamma_w(CH_2)$ progression of bands arising from wagging motions of the lipid methylenes can also be seen between 1180 and 1350 cm^{-1}. This progression of bands is also seen in the dichroic spectrum (Fig. 1, spectrum C), indicating the presence of lipid membranes with acyl chains oriented approximately along the normal to the plate.

The dichroic spectra of apocyt *c* in all membranes studied here showed a positive deviation in the region of the amide I band (≈ 1658 cm^{-1}), as illustrated in Fig. 1 (spectrum C) for apocyt *c* with membranes of DPPG. A positive deviation indicates a net orientation of the dipole moment of the peptide carbonyl bond ($\mu_{C=O}$) perpendicular to the sample plane [24]. Because $\mu_{C=O}$ lies approximately parallel (≈ 27°) to the long axis of the α-helix, the maximum in the amide I region of dichroic spectra of apocyt *c* in lipid membranes suggests that the α-helices in apocyt *c* have a preferential orientation perpendicular to the plane of the membrane. The maximum of the dichroic band was found to be shifted to lower wavenumbers for apocyt *c* with negatively charged lipids (≈ 1656 cm^{-1}) relative to those observed for zwitterionic membranes (≈ 1662 cm^{-1}). This shift suggests that helices contributing to the perpendicular orientation are more stable in negatively charged membranes than in zwitterionic ones.

Deconvoluted FTIR spectra of the amide I band are shown in Fig. 2 for apocyt *c* alone (A) and in the presence of lipid membranes (B and C), before and after 20 min of deuteration. Corresponding spectra of cyt *c* in the absence of lipids are also shown for comparison (D). The maximum of the band occurs ≈ 1650 cm^{-1} for all spectra of deuterated samples, indicating that the main component of secondary structure is the α-helix. Contributions from β-turn can be seen as shoulders around 1675 cm^{-1} in all spectra. A spectral band in the region typical for β-sheet structure is also observed between 1630 and 1635 cm^{-1} in all spectra of deuterated samples. In native cyt *c*, this band has been previously associated with short extended fragments connecting α-helices [25]. The bands at 1624 and 1693 cm^{-1}, observed for apocyt *c* with zwitterionic lipids (Fig. 2B), also fall in the regions characteristic of β-sheet. Analysis of the FTIR spectra revealed a tendency for a higher content of α-helical structure for apocyt *c* in negatively charged lipid membranes (≈ 40 ± 9%), than with zwitterionic membranes (≈ 30 ± 9%), in good agreement with previous results obtained from CD studies [11]. Also, spectra of apocyt *c* alone and with zwitterionic lipids (Fig. 2, spectra A and B) are generally broader than those of apocyt *c* with

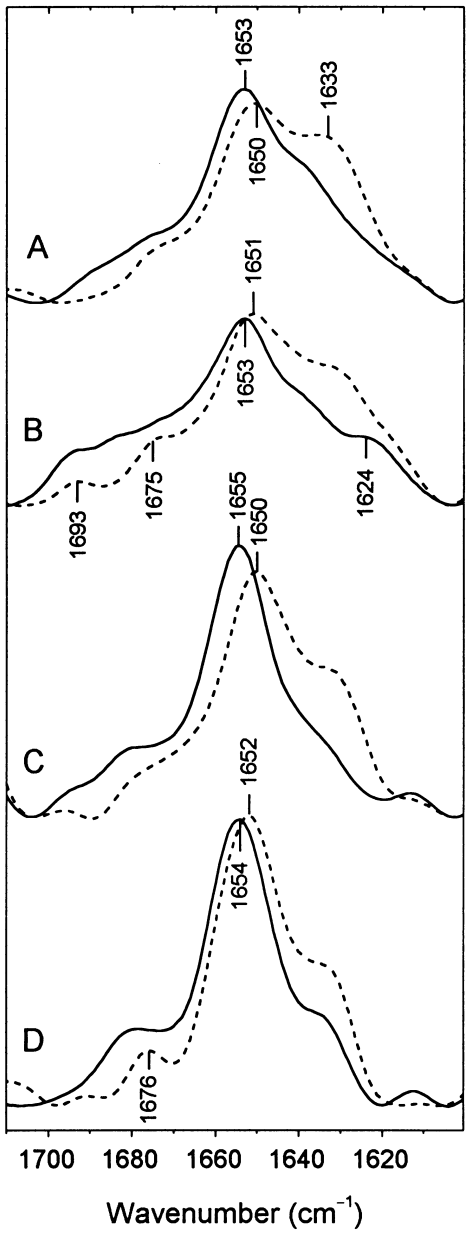

Fig. 2. Normalized amide I region of deconvoluted FTIR spectra. Spectra were obtained for protonated (solid lines) and deuterated (dashed lines) samples of apocyt *c* in the absence of lipids (A), and in the presence of DPPC (B), and DMPG (C). For comparison, spectra for cyt *c* in the absence of lipids are also shown (D). Spectra were recorded with ‖ polarized light, before exposure to D_2O (protonated samples) and after 20 min exposure to D_2O (deuterated samples).

negatively charged membranes (Fig. 2, spectrum C), indicating that the former have larger contributions from secondary structure elements other than α-helix.

H–D exchange kinetics of apocyt *c* amide protons

Amide H–D exchange experiments can provide information on solvent accessibility, hydrogen bonding and general structural stability of proteins. Residues exposed to the solvent, not involved in hydrogen bonds or those in structurally unstable or dynamic regions of proteins will exchange fast. Amide sites in the hydrophobic core of proteins involved in stable hydrogen bonding or buried inside a lipid membrane are more protected from exchange. In the current study, we have investigated the H–D exchange kinetics of partially folded states of apocyt *c* in lipid membranes to gain further insight into their dynamic properties and/or their degree of insertion into the lipid membrane.

The extent of H–D exchange on the protein amide group can be quantitatively evaluated by monitoring the decay in intensity of the amide II band near 1550 cm^{-1} as it shifts by ≈ 100 cm^{-1} towards lower wavenumbers increasing the intensity of the so-called amide II′ band. These changes can be seen in a typical series of spectra recorded during the course of deuteration of apocyt *c* in the presence of DPPG membranes (Fig. 3). The kinetics of H–D exchange for apocyt *c* in lipid membranes, in comparison with the exchange behaviour of apocyt *c* and cyt *c* in the absence of lipids, determined from ‖ spectra, is shown in Fig. 4. Kinetic parameters were determined by non-linear least-square analysis using a minimum number of exponential phases, and a summary of rates and amplitudes is shown in Table 1. Analysis of the H–D exchange kinetics from ⊥ spectra yielded similar results.

The H–D exchange kinetics revealed two main phases: (A) a fast phase with an apparent rate, $k_1 \approx 3$ min^{-1}; and (B) a second phase with a rate $k_2 \approx 0.2$ min^{-1} (Table 1). Because of the deadtime associated with the H–D exchange method in ATR FTIR experiments (≈ 1 min [26]), the rate monitored for the fast phase (k_1) is likely to be faster than that observed and, thus, referred to as an apparent rate. In the absence of lipids, all amide protons in apocyt *c* undergo H–D exchange ($a_D \approx 100\%$; Table 1), while the holoprotein shows a fraction of ≈ 40% of protected amides during the time scale of our measurements (20 min). In the presence of lipids, the total fraction of exchanged residues in apocyt *c* varied between 57 and 88%, depending on the lipid (Table 1). The fraction of fast exchanging amides (a_1) is very similar for cyt *c* and apocyt *c* in the absence of lipid, and decreases for apocyt *c* in lipid

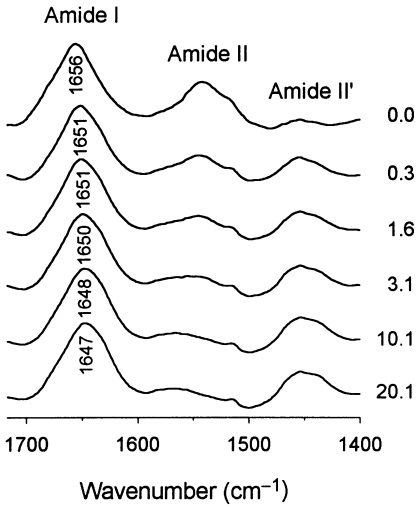

Fig. 3. Typical FTIR spectra recorded using ‖ polarized light during the course of deuteration of apocyt *c* in the presence of DPPG. The time of exposure to D_2O is indicated on the right in minutes. The corresponding lipid background spectra were subtracted from the spectra of the protein–lipid samples.

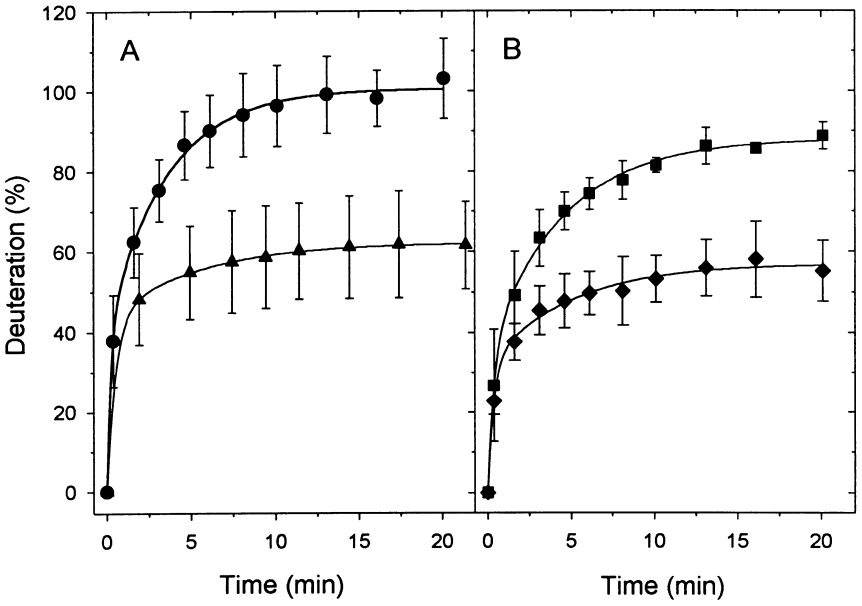

Fig. 4. Deuterated fraction of residues as a function of time of exposure to D_2O. (A) Apocyt *c* (●) and cyt *c* (▲); and (B) apocyt *c* with DMPG (■) and DMPC (◆). Symbols represent mean values of two to three experiments on separate samples with standard deviations shown as error bars. The curves are double exponential fits to the experimental data.

Table 1. H–D exchange kinetic parameters for apocyt *c* and cyt *c* in the presence and absence of membranes. Rates (k_i) and amplitudes (a_i) were measured from the normalized intensity changes of the amide II band of FTIR spectra collected using ‖ polarized light during H–D exchange experiments (see Materials and methods). Amplitudes a_1 and a_2 denote percentage of residues deuterated with rates k_1 and k_2, respectively, a_H is the fraction of non-exchanged residues (protonated) and a_D is the total fraction of exchanged residues (deuterated) calculated as $1-a_H$. Results were obtained by non-linear least-square analysis of mean values of two to three measurements on separate samples. Errors in all parameters represent one standard deviation.

Sample	a_1 (%)	k_1 (min^{-1})	a_2 (%)	k_2 (min^{-1})	a_H (%)	a_D (%)
Cyt *c*	44 ± 3	2.0 ± 0.7	19 ± 2	0.19 ± 0.03	38 ± 1	62 ± 1
Apocyt *c*	40 ± 5	4 ± 1	60 ± 4	0.29 ± 0.03	− 1 ± 1	101 ± 1
Apocyt *c*/DPPG	27 ± 2	3.7 ± 0.5	46 ± 2	0.24 ± 0.02	27 ± 1	73 ± 1
Apocyt *c*/DMPG	35 ± 4	2.8 ± 0.6	53 ± 3	0.22 ± 0.03	12 ± 1	88 ± 1
Apocyt *c*/DPPC	23 ± 7	5 ± 3	36 ± 7	0.42 ± 0.09	41 ± 1	59 ± 1
Apocyt *c*/DMPC	32 ± 4	3.0 ± 0.6	25 ± 3	0.20 ± 0.05	43 ± 1	57 ± 1

membranes. The fraction of amides associated with phase B (a_2) is generally smaller than that observed for apocyt *c* alone, but overall larger than the corresponding fraction for cyt *c* (Table 1).

DISCUSSION

The FTIR spectra of apocyt *c* in zwitterionic and negatively charged lipid membranes revealed that the main component of secondary structure is the α-helix (Fig. 2). Spectral deconvolution showed that negatively charged lipids have a tendency to induce more α-helical structure in apocyt *c* than zwitterionic membranes. This is in good agreement with previous findings of far-UV CD studies in solution [9,11]. However, the broader FTIR spectra observed for apocyt *c* with zwitterionic membranes (Fig. 2B) suggest the presence of other types of secondary structure, likely to be associated with extended β-sheet-like structures. The lower wavenumbers observed for the amide I band in dichroic spectra of apocyt *c* with negatively charged membranes, relative to the values observed with zwitterionic membranes, indicate that the helices with preferential orientation perpendicular to the membrane were more stable in negative lipids than in zwitterionic ones. These differences in stability may be of relevance for the potential role of lipid-associated partially folded states of apocyt *c* in membrane translocation.

The H–D exchange kinetics for native cyt *c* shows that, within the time scale of our measurements (20 min), about 40% of the amide sites remain protected to exchange (Table 1). This is consistent with the existence of a stable hydrophobic core in the native state of cyt *c* [27,28]. In contrast, the complete H–D exchange of apocyt *c* in the absence of lipids indicates that any secondary structure elements present in this state are very unstable (Figs 2 and 4).

The H–D exchange results for apocyt *c* in lipid membranes revealed the existence of three classes of amide protons differing in their H–D exchange kinetics: (A) a group of fast-exchanging amides with an apparent rate (k_1) around 3 min^{-1}; (B) a second group of residues exchanging at a lower rate (k_2) $\approx$ 0.2 min^{-1}; and (C) a third group of amides that did not exchange over 20 min (Table 1). The reduction in the amplitude associated with the fast phase (a_1) in the presence of lipids relative to apocyt *c* or cyt *c* alone suggests that a fraction of this group of amides ($\approx$ 10%) becomes more protected by the lipid environment. The group of fast amides (A) is likely to represent residues exposed to the solvent, not involved in any stable hydrogen bonds, and not protected by the lipid. The protected fraction (C) is probably associated with residues in more structured protein domains or inside the lipid membrane. The

intermediate group of amides (B) would then represent residues involved in weak hydrogen bonds, and not strongly protected by the lipid membrane. Thus, apocyt *c* in the absence of lipids does not have any stable folded structure, but in the presence of lipids 12–43% of residues (depending on the lipid, see Table 1) are involved in more stable structural elements, either buried within the protein or inside the lipid membrane. Alternatively, some of these protected residues may be associated with the β-sheet-like structures observed for apocyt *c* with zwitterionic membranes (Fig. 2, spectrum B).

The positive deviation of the amide I in dichroic spectra indicated that the helices formed in apocyt *c* with lipid membranes have a preferential orientation perpendicular to the plane of the membrane consistent with insertion into the lipid bilayer. Our findings are in good agreement with CD studies by de Jongh *et al*. [13], which revealed that both the N-terminal and C-terminal helices had a favoured orientation perpendicular to the membrane plane of DMPC and DMPG bilayers.

The import of apocyt *c* into mitochondria does not involve the mitochondrial protein translocation machinery [1], and it has been shown that apocyt *c* can insert spontaneously and partially cross the outer mitochondrial membrane [4,5]. Thus, it is tempting to postulate that the unstable and dynamic character of the helices formed in apocyt *c* with lipid membranes could facilitate the process of membrane translocation during import into mitochondria.

In conclusion, we have shown that apocyt *c* acquires a partially folded state upon binding to lipid membranes. In comparison with the unfolded state of apocyt *c* in solution, the main change in secondary structure induced by lipids is associated with an increase in α-helix content. Negatively charged lipid membranes induced larger amounts of α-helical structure than zwitterionic ones. These helices are unstable or very dynamic structures, with a favoured orientation perpendicular to the plane of the lipid membrane. The helices are more stable in negatively charged membranes than those formed in zwitterionic ones. Finally, the observation of a fraction of protected amides varying between 12 and 43% (depending on lipid) indicates the presence of a stable folded domain within the various lipid-associated states of apocyt *c*.

ACKNOWLEDGEMENTS

We thank Dr Kevin Bryson (University of Warwick) for his assistance with the software for spectral analysis, Dr Chris Wharton (University of Birmingham) for critical reading of the manuscript, and Dr Keith Oberg (Université Libre de Bruxelles) for valuable discussion. This work was supported by the Royal Society (grant to T. J. T. P.). E. A. B. and S. E. R. were postdoctoral research fellows under the EC TMR 'Membrane Biogenesis' Network ERBCHRXCT960004 (J.-M. R. and A. W.). T. J. T. P. is a Royal Society University Research Fellow.

REFERENCES

1. Stuart, R.A. & Neupert, W. (1990) Apocytochrome *c*: an exceptional mitochondrial precursor protein using an exceptional import pathway. *Biochimie* **72**, 115–121.
2. Li-Xin, Z., Jordi, W. & de Kruijff, B. (1988). Influence of heme and importance of the N-terminal. *Biochim. Biophys. Acta* **942**, 115–124.
3. Jordi, W., Li-Xin, Z., Pilon, M., Demel, R.A. & de Kruijff, B. (1989) The importance of the amino terminus of the mitochondrial precursor protein apocytochrome *c* for translocation across model membranes. *J. Biol. Chem.* **264**, 2292–2301.
4. Hartl, F.U. & Neupert, W. (1990) Protein sorting to mitochondria: evolutionary conservations of folding and assembly. *Science* **247**, 930–938.
5. Glick, B. & Schatz, G. (1991) Import of proteins into mitochondria. *Annu. Rev. Genet.* **25**, 21–44.
6. Stellwagen, E., Rysavy, R. & Babul, G. (1972) The conformation of horse heart apocytochrome *c*. *J. Biol. Chem.* **247**, 8074–8077.
7. Fisher, W.R., Taniuchi, H. & Anfinsen, C.B. (1973) On the role of heme in the formation of the structure of cytochrome *c*. *J. Biol. Chem.* **248**, 3188–3195.
8. Kuroda, Y. (1993) Residual helical structure in the C-terminal fragment of cytochrome *c*. *Biochemistry* **32**, 1219–1224.
9. De Jongh, H.H.J. & de Kruijff, B. (1990) The conformational changes of apocytochrome *c* upon binding to phospholipid vesicles and micelles of phospholipid based detergents: a circular dichroism study. *Biochim. Biophys. Acta* **1029**, 105–112.
10. Pinheiro, T.J.T., Elöve, G.A., Roder, H., de Jongh, H.H.J., de Kruijff, B. & Watts, A. (1995) Lipid-mediated folding of apocytochrome *c*. *Perspect. Protein Eng. Complementary Technol.* **3**, 62–65.
11. Rankin, S.E., Watts, A. & Pinheiro, T.J.T. (1998) Electrostatic and hydrophobic contributions to the folding mechanism of apocytochrome *c* driven by the interaction with lipid. *Biochemistry* **37**, 37–44.
12. De Jongh, H.H.J., Killian, J.A. & de Kruijff, B. (1992) A water–lipid interface induces a highly dynamic folded state in apocytochrome *c* an cytochrome *c*, which may represent a common fold intermediate. *Biochemistry* **31**, 1636–1643.
13. De Jongh, H.H.J., Brasseur, R. & Killian, J.A. (1994) Orientation of the α-helices of apocytochrome *c* and derived fragments at membrane interfaces, as studied by circular dichroism. *Biochemistry* **33**, 14529–14535.
14. Rankin, S.E., Watts, A., Roder, H. & Pinheiro, T.J.T. (1999) Folding of apocytochrome *c* induced by the interaction with negatively charged lipid micelles proceeds via a collapsed intermediate state. *Protein Sci.* **8**, 381–393.
15. Bryson, E.A., Rankin, S.E., Carey, M., Watts, A. & Pinheiro, T.J.T. (1999) Folding of apocytochrome *c* in lipid micelles: Formation of α-helix precedes membrane insertion. *Biochemistry* **38**, 9758–9767.
16. Brautigan, D.L., Ferguson-Miller, S. & Margoliash, E. (1978) Mitochondrial cytochrome *c*: preparation and activity of native and chemically modified cytochrome *c*. *Methods Enzymol.* **53**, 128–164.
17. Hennig, B. & Neupert, W. (1983) Biogenesis of cytochrome *c* in *Neurospora crassa*. *Methods Enzymol.* **97**, 261–274.
18. Fringeli, U.P. & Günthard, H.H. (1981) Infrared membrane spectroscopy. *Mol. Biol. Biochem. Biophys.* **31**, 270–332.
19. Hübner, W. & Mantsch, H.H. (1991) Orientation of specifically ^{13}C=O labeled phosphatidylcholine multilayers from polarized attenuated total reflection FT-IR spectroscopy. *Biophys. J.* **59**, 1261–1272.
20. Raussens, V., Narayanaswami, V., Goormaghtigh, E., Ryan, R.O. & Ruysschaert, J.-M. (1996) Hydrogen/deuterium exchange kinetics of apolipophorin-III in lipid-free and phospholipid-bound states. *J. Biol. Chem.* **271**, 23089–23095.
21. Kauppinen, J.K., Moffatt, D.J., Cameron, D.G. & Mantsch, H.H. (1981) Noise in Fourier self-deconvolution. *Appl. Optics* **20**, 1866–1879.
22. Goormaghtigh, E., Cabiaux, V. & Ruysschaert, J.-M. (1990) Secondary structure and dosage of soluble and membrane proteins by attenuated total reflection Fourier-transform infrared spectroscopy on hydrated films. *Eur. J. Biochem.* **193**, 409–420.
23. Cabiaux, V., Brasseur, R., Wattiez, R., Falmagne, P., Ruysschaert, J.-M. & Goormaghtigh, E. (1989) Secondary structure of Diptheria toxin and its fragments interacting with acidic liposomes studied by polarized infrared spectroscopy. *J. Biol. Chem.* **264**, 4928–4938.
24. Goormaghtigh, E., Cabiaux, V. & Ruysschaert, J.-M. (1994) Determination of soluble and membrane protein structure by Fourier transform infrared spectroscopy. *Subcell. Biochem.* **23**, 329–450.
25. Byler, M. & Susi, H. (1986) Examination of the secondary structure of proteins by deconvoluted FTIR spectra. *Biopolymers* **25**, 469–487.

26. Goormaghtigh, E., de-Jongh, H.H.J. & Ruysschaert, J.-M. (1996) Relevance of protein thin films prepared for attenuated total reflection Fourier transform infrared spectroscopy: significance of the pH. *Appl. Spectrosc.* **50**, 1519–1527.

27. Roder, H., Elöve, G.A. & Englander, S.W. (1990) Structural characterization of folding intermediates in cytochrome *c* by H-exchange labelling and proton NMR. *Nature (London)* **335**, 700–704.

28. De Jongh, H.H.J., Goormaghtigh, E. & Ruysschaert, J.-M. (1995) Tertiary stability of native and methionine-80 modified cytochrome *c* detected by proton-deuterium exchange using on-line Fourier transform infrared spectroscopy. *Biochemistry* **34**, 172–179.